Surface-enhanced Raman spectroscopy (SERS) characterisation of abasic sites in DNA duplexes

Luca Guerrini, and Ramon A. Alvarez-Puebla.

Abstract

In this study, direct surface-enhanced Raman scattering (SERS) spectroscopy is used as an exquisite nano-optical tool for ultrasensitive structural characterisation of abasic sites in DNA. In addition, the conformational discrimination (intra- vs extra-helical) of the nucleobase opposite to the abasic site was also achieved.

Introduction

Abasic sites, also termed apurinic/apyrimidinic (AP) sites, are non-coding DNA lesions consisting in the loss of a base (while the deoxyribose residue remains in the strand). This class of damages are generated via spontaneous hydrolysis by a variety of chemicals (e.g., reactive oxygen species, alkylating agents), or as intermediates in the base excision repair.1, 2 AP sites facilitate single- and double-stranded breaks which, if not repaired by the base-excision-repair mechanism, lead to mutations.3, 4 The diversity of the biological implications of AP-sites has attracted a great deal of attention. However, while the mutagenic or lethal consequences of persistent AP sites have been detailed, the understanding of their generation, persistence and location within genomic DNA remains inadequate.5

Studies on the impact of abasic sites on the DNA double-helix structures have been carried out to gain insights on the biological role of these lesions. However, the intrinsic instability of the 2-deoxyribose moiety in AP sites largely hinders their structural, thermodynamic and biochemical investigations. To this end, a prototypical abasic residue, the chemically stable 3-hydroxy-2-(hydroxymethyl)tetrahydrofuran, has been typically employed as a reliable AP site analogue of 2'-deoxyribose in the AP site of synthetic oligonucleotides.6 Physicochemical and spectroscopic analyses of these duplexes have been carried out using techniques such as high field NMR spectroscopy, molecular dynamics, fluorescence spectroscopy and calorimetry.2 These studies indicate that AP sites cause a pronounced distortion of the canonical structure at the abasic site while leaving, on the other hand, largely unaltered the overall B-form of the duplex.1, 2, 7 Interestingly, purines bases are preferably incorporated opposite to the abasic site. This has been attributed to their larger free energy of base–base stacking and space-filling ability as compared to pyrimidines, thus increasing the stability of the double-helix.8, 9 On the other hand, adenine insertion is favoured over guanine due to the smaller solvation free energy.1

In the last decade, surface-enhanced Raman spectroscopy (SERS) has emerged as an ultrasensitive tool for the characterisation, detection and quantification of biomolecules.10-13 SERS relies on the plasmon-mediated amplification of the Raman scattering of molecules located at the surface of nanostructured metal substrates to obtain their vibrational fingerprints at very low concentrations.10 In recent years, label-free SERS sensing approaches for nucleic acid analysis have been gaining impulse as a powerful method for their detailed structural characterisation and discrimination.14-21

Nonetheless, to the best of our knowledge, there are no studies reporting the application of SERS to the analysis of abasic sites.

Remarkably, our group has lately developed a new strategy to acquire reliable, reproducible and intense SERS spectra of DNA duplexes (dsDNAs), which has traditionally represented a major obstacle in the implementation of direct SERS to nucleic acid-sensing.14, 22-26 Such an approach relies on the use of spermine-coated silver nanoparticles (AgSp) as efficient plasmonic substrates for nucleic acid detection. Spermine molecules are tetravalent polyamines with high binding affinity for the negatively charged phosphate backbone of DNA, thereby leading to the fast adhesion of the duplexes onto the plasmonic surface regardless of the chain length, sequence and composition (i.e., the double helix conformation hinders the direct interaction of the nucleobases and the plasmonic surface).14 As the DNA molecules act as linkers for nanoparticle aggregation, stable clusters are formed in suspension, sequestering the strands at the interparticle junctions (i.e., electromagnetic hot-spots) and, thus, enabling the acquisition of reliable SERS vibrational fingerprint of the interrogated duplex at low concentrations.14

In this proof-of-concept study, we describe the first example of the application of label-free SERS to the study of different types of AP sites in DNA duplexes. Direct comparison with intact DNA duplexes allows for the identification of the abasic site as well as the recognition of the structural features of the excised nucleobase and its opposite counterpart. Notably, the wealth of vibrational information provided by the acquisition of the DNA SERS fingerprint further enables the characterisation of the intra- vs extra-helical conformation (i.e., stacked vs unstacked) of the nucleobase opposite to the AP site (Fig. 1A).

Cationic silver colloids were prepared by reduction of silver nitrate with sodium borohydride in the presence of spermine tetrahydrochloride.27 The obtained spermine-coated silver nanoparticles (AgSp) display an average 22 nm diameter with a narrow plasmon band centred at ca. 391 nm and a ζ-potential of ca. +40 mV (Fig. 1B).27

Different types of tetrahydrofuran-analogue apurinic and apyrimidinic sites (X) were examined, primarily based on the nature of the opposite base (A, T, G and C). To this end, mutated duplexes (ds1X, ds2X, ds3X, ds4X) were directly compared to the undamaged ones (ds1, ds2, ds3, ds4). Figure 1C shows the corresponding averaged SERS spectra, displaying the characteristic spectral profile of DNA strands hybridized into the double-helix conformation (the full DNA sequences are reported in Fig. S1).22

Most notably, intense and narrow bands in the sub 820 cm-1 spectral range are mainly ascribed to the ring breathing modes of the nucleobases. The relative intensity of these features has been shown to well correlate with the relative nucleobase content.17, 28 Furthermore, these base vibrations are very sensitive to base stacking interactions, whose perturbation of the nucleobase electronic properties determines changes in both peak position and relative intensities of their Raman bands. Specifically, a general blue-shift of the ring breathing modes is observed upon strand hybridization,22 while normal Raman studies of melting duplexes showed a decrease in Raman intensity upon the formation of stacked base structures.29 On the opposite side of the spectral range (ca. 1150-1720 cm-1), we find an ensemble of overlapping bands mainly due to in-plane ring vibrations of the nucleobases, and an additional broad feature centred around 1650 cm-1

which is ascribed to the collection of carbonyl stretching modes. This latter band provides a spectral marker of H-bonding interactions, undergoing a large red-shift upon base pairing.22 Finally, in the intermediate spectral range (820–1150 cm-1), the SERS spectra reveal a set of relatively weak bands arising from the deoxyribose-linked phosphodiester network, with the exception of the intense feature at ca. 1090 cm-1 due to the symmetric stretching of the phosphodioxy moiety. This vPO2- band is largely insensitive to the DNA structural changes and, thus, has been typically exploited as an internal standard in vibrational studies.14, 28

As expected from dsDNA with such high structural similarity, SERS spectra display a significant degree of resemblance. Thus, difference spectra were obtained to fully unveil the spectral discrepancies via digital subtraction of the SERS of the AP-site containing dsDNAs (ds1X, ds2X, ds3X and ds4X) to those of the corresponding fully matched duplexes (ds1, ds2, ds3 and ds4). The difference spectra are illustrated in Fig. 2A and 3, together with the SERS of reference homopolymeric single-stranded DNAs (ssA, ssC, ssT and ssG) and fully matched dsDNA containing only C+G or A+T nucleobases in a 1:1 ratio (dsCG and dsAT, respectively. See Fig. S1 for the detailed sequences of the reference DNA samples). The solution of the homopolymeric single-stranded ssG was thermally treated prior to the SERS measurements to disrupt multiple-stranded secondary structures promoted by G-quadruplex formation and, thus favor the extension of the ssG molecules and their interaction with the metal surface.25 All difference spectra display a set of positive features corresponding to the additional nucleobase contained in the fully matched duplexes, among others: (i) ds1–ds1X, bands at ca. 730, 1321, and 1507 cm-1, attributed to A; (ii) ds2–ds2X, bands at ca. 786, 1244, 1486, and 1526 cm-1 corresponding to C; (iii) ds3–ds3X, bands at ca. 787 and 1369 cm-1, ascribed to T; and (iv) ds4–ds4X, bands at ca. 674 and 1347 cm-1, assigned to G. As a result, we can therefore indirectly infer the nature of the complementary nucleobase removed at the abasic site (i.e., A, C, T and G, respectively).

Interestingly, the positive features in the difference spectra corresponding to the ring breathing modes have the same peak position of those involved in the ds4G and ds3T duplexes (786 cm-1 for C, 673 cm-1 for G, 730 cm-1 for A, and 787 cm-1 for T) which are blue-shifted as compared to those of the homopolymeric single strands (790 cm-1 for C, 684 cm-1 for G, 734 cm-1 for A, and 790 cm-1 for T) (Fig. 2 and 3). Thus, direct SERS analysis of DNA with AgSp is capable of identifying single nucleobases mismatches and discriminating base conformation (i.e., unpaired vs paired).

Remarkably, ds4–ds4X difference spectrum also clearly displays negative features which appear to correspond to C (786 and 1247 cm-1). The additional presence of these negative contributions can be understood based on the disruptive effect that AP sites have on the structure of neighbouring base pairs, which largely depends on the nature of the flanking and opposite bases.1, 2, 8, 30-32 Typically, a purine base (A, G) facing an AP site retains the regular right-handed DNA geometry, thereby remaining stacked within the helix. On the other hand, intra- and extra-helical configurations can be adopted by pyrimidines (C, T), depending on the chemical nature of the abasic site and the flanking bases.2, 33 In particular, molecular dynamics simulations indicate that, under the investigated conditions (temperature), samples with adenines as AP site flanking bases (A-X-A, Fig. 1C) favour the extra-helical displacement of the opposite pyrimidine bases (C, T).30 This has been ascribed to the stronger purine-purine stacking interactions which

lead to the approaching of the distant adenines, the contraction of the AP site and, finally, the expulsion of the opposite pyrimidine bases.8 The experimental outcome of the SERS spectra can be then interpreted accordingly. In the case of ds4–ds4X, the negative feature at ca. 789 cm-1 can be recognized as the spectral marker of the extrahelical conformation of the C opposite to the abasic site, as indicated by both its increase in Raman intensity and spectral redshift which are informative of the unstacked C form (Fig. 2B). The ds1–ds1X difference spectrum also reveals a negative feature centred at ca. 792 cm-1, which could suggest the presence of a T nucleobase in a preferably extrahelical conformation, in agreement with the previous considerations (Fig. 3). However, in this case, the spectral variation of the thymine ring breathing band is much less explicit as compared to C, possibly due to the much larger Raman cross-section of the additional base (A) as compared to the opposite T,34 which makes the thymine features far less distinguishable in the difference spectrum.

In summary, we have first described the application of direct SERS analysis to the spectral study of abasic sites in duplexes DNA. Identification of the nucleobase lesion is achieved at the single-base level by direct comparison with the unmodified duplex. In particular, the ring breathing modes generate narrow and intense bands providing spectral markers not only for the discrimination of excised nucleobase at the AP lesion but also features informative of the intra- vs extra-helical conformation of the base opposite to the abasic site.

Funding

This work was funded by the Spanish Ministerio de Economía, Industria y Competitividad (CTQ2017-88648R, RYC-2016-20331), the Generalitat de Cataluña (2017SGR883), the Universitat Rovira i Virgili (2018PFRURV-B2-02), and the Universitat Rovira i Virgili and Banco Santander (2017EXIT-08).

Notes and references

1. D. M. Wilson and D. Barsky, *Mut. Res. DNA Repair*, 2001, **485**, 283-307.
2. J. Lhomme, J. F. Constant and M. Demeunynck, *Biopolymers*, 1999, **52**, 65-83.
3. J. Malina and V. Brabec, *Chem.-Eur. J.*, 2014, **20**, 7566-7570.
4. L. A. Loeb and B. D. Preston, *Annu. Rev. Genet.*, 1986, **20**, 201-230.
5. Z. J. Liu, S. Martínez Cuesta, P. van Delft and S. Balasubramanian, *Nat. Chem.*, 2019, **11**, 629-637.
6. M. Takeshita, C. N. Chang, F. Johnson, S. Will and A. P. Grollman, *J. Biol. Chem.*, 1987, **262**, 10171-10179.
7. G. Vesnaver, C. N. Chang, M. Eisenberg, A. P. Grollman and K. J. Breslauer, *Proc. Natl. Acad. Sci. U.S.A.*, 1989, **86**, 3614-3618.
8. P. Cuniasse, G. V. Fazakerley, W. Guschlbauer, B. E. Kaplan and L. C. Sowers, *J. Mol. Biol.*, 1990, **213**, 303-314.
9. C. A. Gelfand, G. E. Plum, A. P. Grollman, F. Johnson and K. J. Breslauer, *Biochemistry*, 1998, **37**, 7321-7327.
10. S. Schlücker, *Angew. Chem.-Int. Edit.*, 2014, **53**, 4756-4795.
11. C. Zong, M. X. Xu, L. J. Xu, T. Wei, X. Ma, X. S. Zheng, R. Hu and B. Ren, *Chem. Rev.*, 2018, **118**, 4946-4980.
12. S. Laing, L. E. Jamieson, K. Faulds and D. Graham, *Nat. Rev. Chem.*, 2017, **1**, 0060.
13. L. Guerrini and R. A. Alvarez-Puebla, *Cancers*, 2019, **11**, 748.
14. E. Garcia-Rico, R. A. Alvarez-Puebla and L. Guerrini, *Chem. Soc. Rev.*, 2018, **47**, 4909-4923.
15. Y. Li, T. Gao, G. Xu, X. Xiang, X. Han, B. Zhao and X. Guo, *J. Phys. Chem. Lett.*, 2019, **10**, 3013-3018.
16. J. Morla-Folch, P. Gisbert-Quilis, M. Masetti, E. Garcia-Rico, R. A. Alvarez-Puebla and L. Guerrini, *Angew. Chem.-Int. Edit.*, 2017, **56**, 2381-2385.
17. J. Morla-Folch, R. A. Alvarez-Puebla and L. Guerrini, *J. Phys. Chem. Lett.*, 2016, **7**, 3037-3041.

18. K. M. Koo, J. Wang, R. S. Richards, A. Farrell, J. W. Yaxley, H. Samaratunga, P. E. Teloken, M. J. Roberts, G. D. Coughlin, M. F. Lavin, P. N. Mainwaring, Y. Wang, R. A. Gardiner and M. Trau, *ACS Nano*, 2018, **12**, 8362-8371.
19. S. Dick, S. E. J. Bell, K. J. Alexander, I. A. O'Neil and R. Cosstick, *Chem. Eur. J.*, 2017, **23**, 10663-10669.
20. J. Wang, K. M. Koo, E. J. H. Wee, Y. Wang and M. Trau, *Nanoscale*, 2017, **9**, 3496-3503.
21. E. Papadopoulou and S. E. J. Bell, *Angew. Chem.-Int. Edit.*, 2011, **50**, 9058-9061.
22. L. Guerrini, Ž. Krpetić, D. van Lierop, R. A. Alvarez-Puebla and D. Graham, *Angew. Chem.-Int. Edit.*, 2015, **54**, 1144-1148.
23. M. Masetti, H.-n. Xie, Ž. Krpetić, M. Recanatini, R. A. Alvarez-Puebla and L. Guerrini, *J. Am. Chem. Soc.*, 2015, **137**, 469-476.
24. J. Morla-Folch, H.-n. Xie, P. Gisbert-Quilis, S. Gómez-de Pedro, N. Pazos-Perez, R. A. Alvarez-Puebla and L. Guerrini, *Angew. Chem.-Int. Edit.*, 2015, **54**, 13650-13654.
25. A. Torres-Nunez, K. Faulds, D. Graham, R. A. Alvarez-Puebla and L. Guerrini, *Analyst*, 2016, **141**, 5170-5180.
26. P. Gisbert-Quilis, M. Masetti, J. Morla-Folch, J. M. Fitzgerald, N. Pazos-Perez, E. Garcia-Rico, V. Giannini, R. A. Alvarez-Puebla and L. Guerrini, *Adv. Mater. Interfaces*, 2017, **4**, 1700724.
27. D. van Lierop, Z. Krpetic, L. Guerrini, I. A. Larmour, J. A. Dougan, K. Faulds and D. Graham, *Chem. Commun.*, 2012, **48**, 8192-8194.
28. L.-J. Xu, Z.-C. Lei, J. Li, C. Zong, C. J. Yang and B. Ren, *J. Am. Chem. Soc.*, 2015, **137**, 5149-5154.
29. P. Y. Turpin, L. Chinsky, A. Laigle and B. Jolles, *J. Mol. Struct.*, 1989, **214**, 43-70.
30. P. Cuniasse, L. C. Sowers, R. Eritja, B. Kaplan, M. F. Goodman, J. A. H. Cognet, M. LeBret, W. Guschlbauer and G. V. Fazakerley, *Nucleic Acids Res.*, 1987, **15**, 8003-8022.
31. M. P. Singh, G. C. Hill, D. Peoc'h, B. Rayner, J.-L. Imbach and J. W. Lown, *Biochemistry*, 1994, **33**, 10271-10285.
32. K. M. Morden, Y. G. Chu, F. H. Martin and I. Tinoco, *Biochemistry*, 1983, **22**, 5557-5563.
33. M. Lukin and C. de los Santos, *Chem. Rev.*, 2006, **106**, 607-686.
34. A. Barhoumi, D. Zhang, F. Tam and N. J. Halas, *J. Am. Chem. Soc.*, 2008, **130**, 5523-5529.

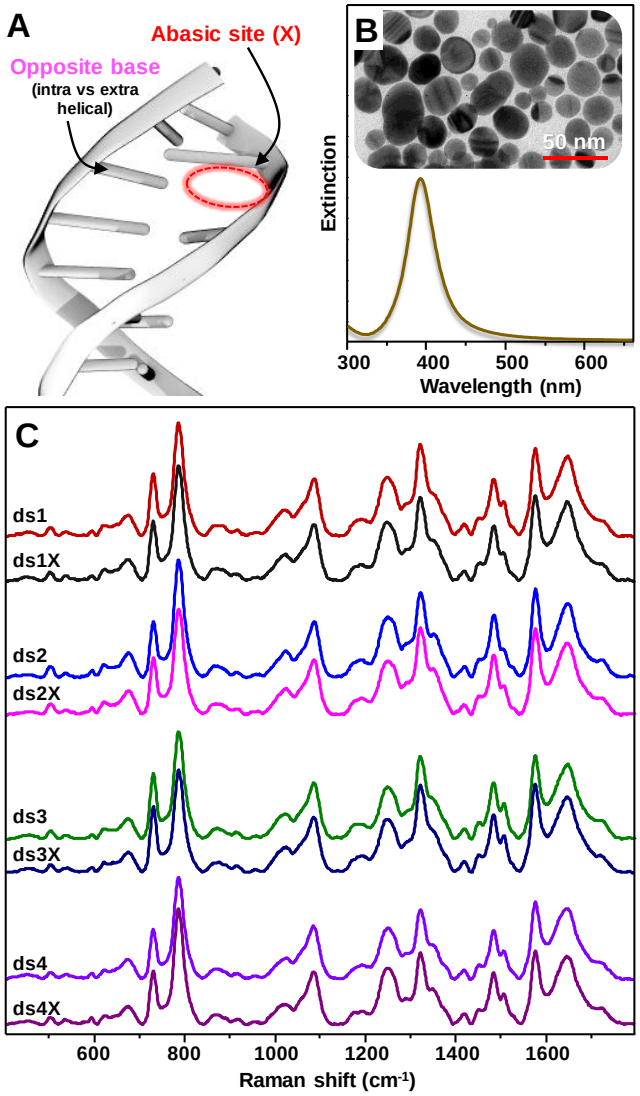

ds1 = AGTCGTATCCGAG / TCAGCATAGGCTC

ds1X = AGTCGTXTCCGAG / TCAGCATAGGCTC

ds2 = AGTCGTCTCCGAG / TCAGCAGAGGCTC

ds2X = AGTCGTXTCCGAG / TCAGCAGAGGCTC

ds3 = AGTCGTTTCCGAG / TCAGCAAAGGCTC

ds3X = AGTCGTXTCCGAG / TCAGCAAAGGCTC

ds4 = AGTCGTGTCCGAG / TCAGCACAGGCTC

ds4X = AGTCGTXTCCGAG / TCAGCACAGGCTC

Figure 1. (A) Schematic outline of the abasic site within duplex. (B) Extinction spectrum of AgSp colloids and a representative TEM image of the silver nanoparticles. (C) SERS spectra of the double-stranded DNA samples. Base sequences at the abasic site are also illustrated. Spectra were normalized to the vPO_2^- band at 1090 cm^{-1}. DNA sequences are shown at the bottom.

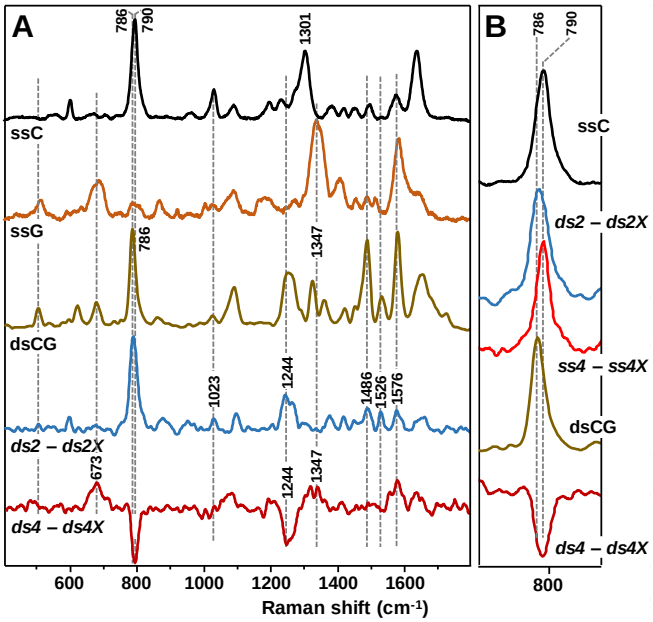

Figure 2. (A) SERS spectra of the reference samples: single-stranded ssC and ssG, and double-stranded ds4G. Digitally subtracted SERS spectra *ds2 – ds2X*, and *ds4 – ds4X*. (B) Detail of the cytosine ring breathing spectral region. SERS spectra of the reference samples: single-stranded ssC and ssG, and double-stranded dsCG. Digitally subtracted SERS spectra *ds2 – ds2X*, and *ssC – ssX*. Single strand sequences: ss4 = AGTCGTCTCCGAG; ss4X = AGTCGTXTCCGAG.

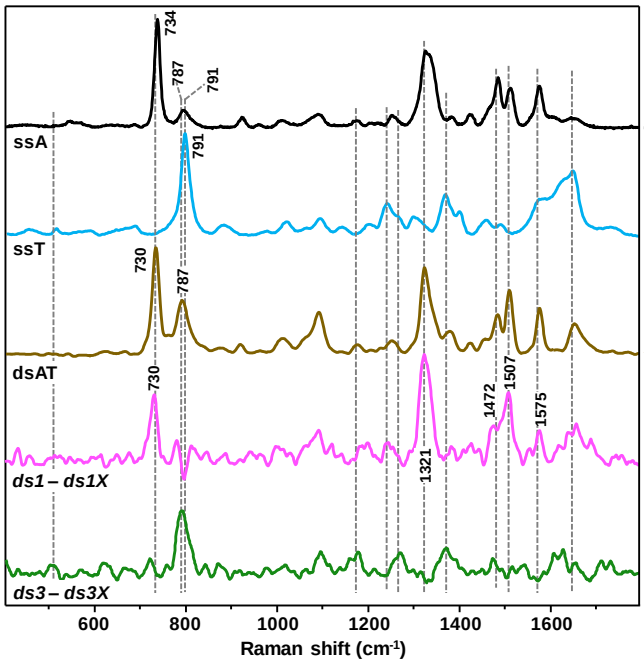

Figure 3. SERS spectra of the reference samples: single-stranded ssA and ssT, and double-stranded dsAT. Digitally subtracted SERS spectra *ds1 – ds1X*, and *ds3 – ds3X*.